Broken symmetries and pattern formation in two-frequency forced Faraday waves

Jeff Porter* and Mary Silber
Department of Engineering Sciences and Applied Mathematics, Northwestern University, Evanston, Illinois 60208
(Dated: February 8, 2008)

We exploit the presence of approximate (broken) symmetries to obtain general scaling laws governing the process of pattern formation in weakly damped Faraday waves. Specifically, we consider a two-frequency forcing function and trace the effects of time translation, time reversal and Hamiltonian structure for three illustrative examples: hexagons, two-mode superlattices, and two-mode rhomboids. By means of explicit parameter symmetries, we show how the size of various three-wave resonant interactions depends on the frequency ratio m:n and on the relative temporal phase of the two driving terms. These symmetry-based predictions are verified for numerically calculated coefficients, and help explain the results of recent experiments.

PACS numbers: 47.54.+r, 05.45.-a, 47.35.+i, 47.20.Gv

Symmetry arguments play a central role in our understanding of pattern formation in nonlinear, nonequilibrium systems. They explain, for example, the ubiquity of simple patterns such as hexagons, squares and stripes observed in widely disparate systems, both in nature and in the laboratory [1]. Group theory provides the natural language for describing and classifying patterns and, when combined with bifurcation theory, it determines which patterns may result from a symmetry-breaking instability [2]. It is by now standard practice to invoke symmetry arguments to determine which nonlinear terms are present in the universal amplitude equations that govern the pattern formation processes near onset. The detailed physics is manifest in these amplitude equations only through the numerical values of the coefficients of the nonlinear terms, yet the computation of these coefficients is often an arduous task that must be carried out numerically.

In this letter we develop symmetry arguments in a somewhat nonstandard way, using *parameter symmetries* (symmetries which act on both amplitudes and parameters; see e.g. [3]) to determine the dependence of the most important *coefficients* in the amplitude equations on the parameters of the forcing function and on the damping. The specific problem we consider is that of gravity-capillary wave excitation on the free surface of a fluid subjected to the (vertical) forcing function

$$F(t) = \frac{1}{2}(f_m e^{im\omega t} + f_n e^{in\omega t} + cc.) \equiv |f_m|\cos(m\omega t + \phi_m) + |f_n|\cos(n\omega t + \phi_n), \quad (1)$$

where m and n are relatively prime. This system, with its wealth of readily tuneable control parameters, has been a rich source of intriguing patterns [4, 5, 6, 7, 8]. Although a variety of nonlinear interactions influence the pattern selection process, resonant triads are especially important because they arise at second order in a weakly-nonlinear expansion and lead to a strong phase coupling between the three waves involved - they have been implicated in many Faraday wave pattern studies, both experimental [6, 7, 8] and theoretical [9, 10]. This letter uses general symmetry arguments applied to several such three-wave interactions to shed some light on the role of the control parameters ($|f_m|$, $|f_n|$, $m\omega$, $n\omega$, ϕ_m, ϕ_n) in the pattern formation process.

Symmetry considerations, both spatial and temporal, have already gone a long way toward elucidating the general mechanisms by which different patterns arise. For example, when a *single* frequency ω is used, a sufficiently large forcing excites standing waves (SW) with primary frequency $\omega/2$. After one period T of the driving, the SW eigenmodes ψ_j are exactly out of phase and, due to the symmetry $t \to t+T$, $\psi_j \to -\psi_j$, are barred from quadratic (i.e. three-wave) interactions. The addition of a second commensurate frequency (when not a multiple of the first) breaks this particular discrete translation symmetry and replaces it with one on a *longer* timescale: $t \to t + pT$. If p is even this weaker symmetry constraint permits three-wave interactions by recasting the ψ_j as *harmonic* modes. Despite the success of this argument in explaining the emergence of hexagons when a second frequency is added [4] it fails to predict either the size of the symmetry-breaking effect or its dependence on the control parameters.

In this letter we take advantage of nearby (approximate) symmetries to make further progress. The main idea is that, for weakly-damped small-amplitude dynamics, the real physical system (damped forced SW) is intimately related to an underlying system (undamped unforced traveling waves (TW)) that is subject to more stringent symmetry requirements: invariance under *arbitrary* time translations $t \to t+\tau$, and time reversal $t \to -t$. If the undamped but forced problem is Hamiltonian the system is still further constrained. Although the addition of forcing and damping destroys these symmetries, their influence persists. In fact, the broken symmetries can be replaced by corresponding parameter symmetries which remain intact for *any* damping and forcing. It

is only to obtain useful scaling laws that we must restrict ourselves to *small* damping and forcing.

The overall strategy is illustrated in Fig. 1. First, we

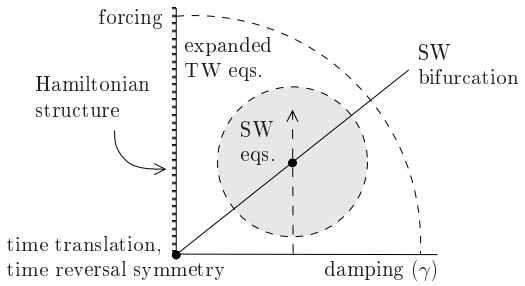

FIG. 1: Relationship of SW equations to underlying symmetries. The origin denotes systems with time translation and time reversal symmetry. The undamped problem is Hamiltonian. SW bifurcate from the flat state along the solid line, while the dashed vertical line illustrates a realistic experimental path.

express physical variables such as surface height $h(\boldsymbol{x},t)$ in terms of the TW eigenfunctions of the undamped unforced problem:

$$h(\boldsymbol{x},t)=\sum_{j=1}^{N}\sum_{\pm} Z_j^{\pm}(t)\,e^{i(\boldsymbol{k}_j\cdot\boldsymbol{x}\pm\Omega_j t)}+cc.+\dots . \qquad (2)$$

In all cases N is finite (we consider only periodic patterns). Evolution equations for the TW amplitudes $Z_j^{\pm}$ must respect the appropriate spatial symmetries, which depend on the planform considered, and the following parameter symmetries:

$$T_\tau\colon Z_j^{\pm}\to e^{\pm i\Omega_j\tau}Z_j^{\pm},\ (f_m,f_n)\to(f_m e^{im\tau},f_n e^{in\tau}),$$
$$\kappa: Z_j^{\pm}\leftrightarrow Z_j^{\mp},\ (t,\gamma)\to-(t,\gamma),\ (f_m,f_n)\to(\bar f_m,\bar f_n). \quad (3)$$

Here $\gamma=2\nu k^2/\omega$ is a dimensionless damping parameter (ν denotes viscosity and $k(\omega)$ is a characteristic wavenumber). Next, we assume the TW equations can be expanded in powers of γ, f_m and f_n and so determine their form for small damping and forcing. Lastly, these expanded TW equations are reduced at the primary bifurcation through a center manifold reduction to yield the equations describing SW near onset. The procedure outlined above can be applied to numerous patterns and we shall look briefly at three: hexagons, two-mode superlattices [7], and two-mode rhomboids [6]. We test the predicted dependence of SW coefficients by numerically calculating them from the Zhang-Viñals model [9], a quasipotential formulation of the Faraday problem appropriate for a deep layer of nearly inviscid fluid. This reduction (see [10]) is done directly at the primary bifurcation to SW and does not rely on the symmetry arguments we develop here.

I. **Simple hexagons**. These common patterns are favored by quadratic interactions requiring harmonic eigenmodes. We therefore take the coprime integer associated with the instability (n, say) to be even, and set $N=3$, $\Omega_1=\Omega_2=\Omega_3=n\omega/2$ in the TW expansion (2). The neutral stability curves in the (k,f) plane ($f^2\equiv|f_m|^2+|f_n|^2$) might resemble the sketch in Fig. 2b.

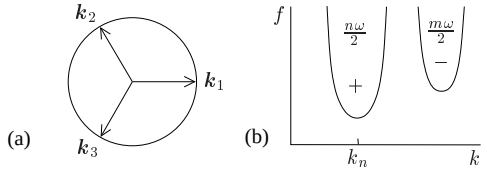

FIG. 2: Simplified sketch of when hexagons arise. With n even the modes excited by f_n are harmonic (labeled "+") and those excited by f_m are subharmonic ("−").

Spatial symmetries (translation, reflection, and 60° rotation) in combination with Eqs. (3) lead to

$$\dot Z_1^{+}=\upsilon Z_1^{+}-\tilde\mu f_n Z_1^{-}+\varpi(Z_2^{+}\bar Z_2^{-}+Z_3^{+}\bar Z_3^{-})Z_1^{-}$$
$$+\begin{Bmatrix}\tilde\beta f_m^{\frac{n}{2}}(\bar Z_2^{+}\bar Z_3^{-}+\bar Z_2^{-}\bar Z_3^{+})+\tilde\gamma\bar f_m^{\frac{n}{2}}\bar Z_2^{-}\bar Z_3^{-}, & m=1\\ \tilde\alpha f_m^{\frac{n}{2}}\bar f_n^{\frac{m-3}{2}}\bar Z_2^{+}\bar Z_3^{+}, & m>1\end{Bmatrix}$$
$$+Z_1^{+}\sum_{j,\pm}\tilde a_j^{\pm}|Z_j^{\pm}|^2. \qquad (4)$$

The other five equations follow from symmetry. At each order in amplitude, up to third order, the leading order terms (in f_m, f_n, γ) have been kept. Terms of order $|Z|^3 f$ are neglected here (and in the examples that follow) because they produce no new qualitative effects. Note that the quadratic terms in Eqs. (4) split into two cases: $m=1$ and $m>1$. The time reversal symmetry κ in (3) forces most of the coefficients to be imaginary at leading order. For example, we may write

$$\tilde\mu=\tilde\mu_r\gamma+i(\tilde\mu_i+\tilde\mu_m|f_m|^2+\tilde\mu_n|f_n|^2+\tilde\mu_\gamma\gamma^2)+\dots . \quad (5)$$

Here $\tilde\mu_r,\tilde\mu_i$, etc. are real and, with an appropriate sign convention for the forcing term in the governing equations, we can take $\tilde\mu_i>0$. The only coefficient which does not submit to a simple transcription of Eq. (5) is υ because, having chosen the wavevectors of the expansion to lie on the critical circle (itself a function of γ), we must have the detuning, $\mathrm{Im}(\upsilon)$, vanish at $\gamma=f=0$.

At the bifurcation to SW, eigenvectors take the form $Z_j^{\pm}=e^{\pm i\varphi}A_j$ where $\varphi=\phi_n/2-\pi/4+\mathcal{O}(\gamma)$. A center manifold reduction yields

$$\dot A_1=\mu A_1+\alpha\bar A_2\bar A_3+A_1\left(a|A_1|^2+b|A_2|^2+b|A_3|^2\right), \quad (6)$$

with equations for A_2 and A_3 obtained by cyclic permutation. The normal form coefficients are given (to lowest order) by

$$\alpha=-|f_m|^{\frac{n}{2}}\begin{Bmatrix}(2\tilde\beta_i-\tilde\gamma_i)\sin\Phi, & m=1\\ \tilde\alpha_i|f_n|^{\frac{m-3}{2}}\cos\Phi, & m>1\end{Bmatrix},\quad a=C_1\gamma,$$
$$b=C_2\gamma+\frac{|f_m|^n}{\gamma}\begin{Bmatrix}C_3\cos^2\Phi, & m=1\\ -|C_4||f_n|^{m-3}\sin^2\Phi, & m>1\end{Bmatrix}. \quad (7)$$

Here $\Phi = \pi/4 - \phi_f/2$ with $\phi_f \equiv m\phi_n - n\phi_m$ (this is the only linear combination of ϕ_m and ϕ_n which cannot be set arbitrarily just by redefining the origin in time). The C_j are known functions of υ_r, $\tilde{\mu}_m$, etc., independent of f_m, f_n, γ (see [11]). Note that α inherits the f_m, f_n dependence of the corresponding resonant term in Eqs. 4 and, since at the bifurcation to SW we have $|f_n|, |f_m| \sim \gamma$, it follows that α scales as $\gamma^{n/2}$ if $m = 1, 3$ and $\gamma^{(n+m-3)/2}$ otherwise. Furthermore, α has a simple harmonic dependence on the T_τ-invariant phase Φ. Both of these predictions are borne out in Fig. 3 for several values of m:n. This figure also illustrates how the oscillations in α can lead to oscillations in the range of forcing amplitude over which hexagons are stable. Similar oscillations have been seen experimentally [4, 5]. One can understand such behavior as follows: while the linear eigenmodes are phase-locked to the forcing f_n which parametrically excites them, the nonlinear forcing from the resonant terms (which involves f_m) attempts to induce a different temporal phase. These two influences may cooperate or compete, depending on the relative phase ϕ_f.

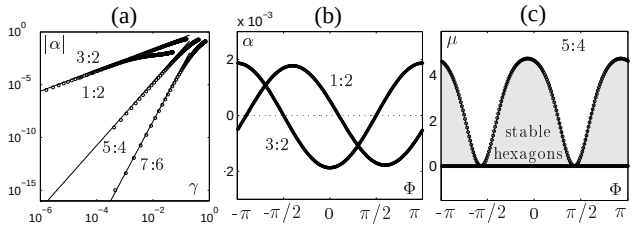

FIG. 3: Numerical calculations based on the Zhang Viñals equations (for a summary of the procedure see [10]). (a) $|\alpha(\gamma)|$ for several choices of m:n [12]. Solid lines show predicted scalings. (b) $\alpha(\Phi)$ for m:n = 1:2 and 3:2, both with $\gamma \simeq 0.001$. These cases have identical scaling in γ but are phase-shifted in Φ. (c) Range of stable hexagons in Eqs. (6) for m:n = 5:4 and (realistic) parameters such that $\gamma \simeq 0.245$.

II. **Two-mode superlattices (2MS)**. These were observed with almost all forcing ratios by Arbell and Fineberg [6, 8] near the *bi-critical* point where the two modes driven by f_m and f_n onset simultaneously. The relevant three-wave interaction also includes a third linearly damped mode (see Fig. 4b) with predominant oscillations at half the "difference frequency". The 2MS states typically emerge from an underlying square or hexagonal lattice and involve multiple resonant triads [6, 8]. For simplicity, we focus here on a single characteristic triad (Fig. 4a), i.e., we treat an invariant subspace of the full 2MS problem. A combination of spatial and temporal symmetries (3) again determines the form of the six TW evolution equations. In the vicinity of the bi-critical point these TW equations reduce to SW equations

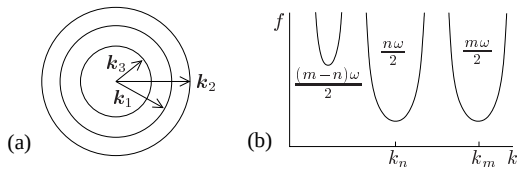

FIG. 4: Sketch of the linear problem for 2MS. We take $m > n$.

$$\dot{A}_1 = \lambda A_1 + A_1\left(a|A_1|^2 + b|A_2|^2\right),$$
$$\dot{A}_2 = \mu A_2 + A_2\left(c|A_1|^2 + d|A_2|^2\right), \qquad (8)$$

with coefficients of the form

$$\begin{pmatrix} a \\ b \\ c \\ d \end{pmatrix} = \begin{pmatrix} C_1 \\ C_2 \\ C_3 \\ C_4 \end{pmatrix} \gamma + \begin{pmatrix} 0 \\ |C_5|\tilde{\beta}_i\tilde{\kappa}_i \\ -|C_5|\tilde{\alpha}_i\tilde{\kappa}_i \\ 0 \end{pmatrix} \frac{1}{\gamma}. \qquad (9)$$

Here the C_j are known functions, independent of γ, f_m, and f_n while $\tilde{\alpha}_i$, $\tilde{\beta}_i$, and $\tilde{\kappa}_i$ are the imaginary parts of the quadratic resonant coefficients in $\dot{Z}_1^+$, $\dot{Z}_2^+$, and $\dot{Z}_3^+$, respectively. The most important effect of Hamiltonian structure on the TW equations comes via these last three coefficients. Specifically, if at $\gamma = 0$ there exists a Hamiltonian $\mathcal{H}$ such that $dZ_j^\pm/dt = \mp i\partial\mathcal{H}/\partial\bar{Z}_j^\pm$, then $\tilde{\alpha}_i = \tilde{\beta}_i = \tilde{\kappa}_i$. The equality here is an overstatement since the equations (and hence the coefficients) can always be rescaled. One expects simply $\tilde{\alpha}_i \sim \tilde{\beta}_i \sim \tilde{\kappa}_i$ and thus, for small damping, $1 \ll b \sim -c$. If, in addition, both primary bifurcations (to pure modes) within Eqs. (8) are supercritical then $0 < -a \sim -d \ll 1$. Under these conditions stable 2MS states (mixed states within Eqs. (8)) inhabit the region shown in Fig. 5a. This region agrees quite well with the experiments of Arbell and Fineberg [6] despite being based on a simplified version of the 2MS states. The indifference of Eqs. (9) to m and n helps explain why 2MS patterns were observed for virtually all forcing ratios [6].

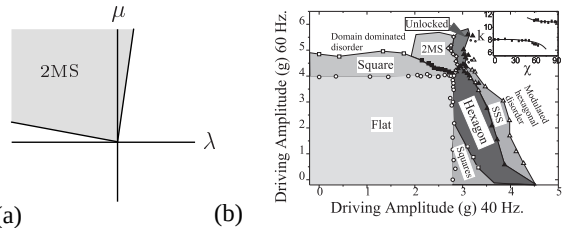

FIG. 5: (a) Region of stable 2MS under the assumptions of small damping, Hamiltonian structure, and supercriticality, (b) Experimental data, courtesy of J. Fineberg, reproduced from [6]. Since $\lambda \sim |f_n| - |f_n|^{\rm crit}$ and $\mu \sim |f_m| - |f_m|^{\rm crit}$ the orientation of the axes in (a) and (b) is the same.

III. **Two-mode rhomboids (2MR)**. These patterns are found [7] near the bi-critical point but, unlike 2MS, do not rely on damped modes; see Fig. 6. As before,

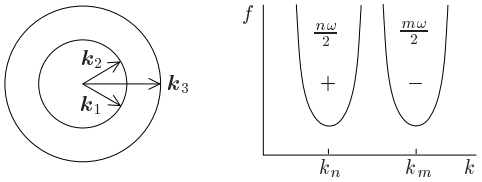

FIG. 6: Sketch of the linear picture for 2MR. We take m odd and n even.

spatial symmetries and Eqs. (3) determine the form of the six TW equations that reduce to SW equations at the bi-critical point:

$$\dot{A}_1 = \lambda A_1 + \alpha \bar{A}_2 A_3 + A_1\big(a|A_1|^2 + b|A_2|^2 + c|A_3|^2\big),$$
$$\dot{A}_3 = \mu A_3 + \beta A_1 A_2 + A_3\big(d|A_1|^2 + d|A_2|^2 + e|A_3|^2\big), \quad (10)$$

with resonant coefficients of the form

$$\begin{pmatrix} \alpha \\ \beta \end{pmatrix} = \begin{pmatrix} \tilde{\alpha}_i \\ -\tilde{\beta}_i \end{pmatrix} |f_m|^{\frac{n-2}{2}} |f_n|^{\frac{m-1}{2}} \cos\Phi. \quad (11)$$

Again $\Phi = \pi/4 - \phi_f/2$ with $\phi_f = m\phi_n - n\phi_m$. Hamiltonian structure at $\gamma = 0$ implies $\tilde{\alpha}_i \sim \tilde{\beta}_i$ and thus $\tilde{\alpha}_i\tilde{\beta}_i > 0$, or equivalently, $\alpha\beta < 0$ (see [13] for proof of an analogous relation in a class of self-adjoint hydrodynamic problems). The condition $\alpha\beta < 0$ has enormous dynamical consequences for Eqs. (10) and is associated with the presence of modulated drifting waves and heteroclinic cycles [11, 14]. We have confirmed the opposing signs of α and β, as well as the predicted scaling $|\alpha|$, $|\beta| \sim \gamma^{(m+n-3)/2}$, for a wide range of forcing ratios by numerically calculating these coefficients from the Zhang-Viñals equations. The exponential decrease of $|\alpha|$ and $|\beta|$ with $m+n$ helps explain why 2MR have been seen in [7, 8] for m:n = 3:2 and 5:4 but not with higher values of $m+n$; for m:n = 1:2 the same three-wave resonance is observed, but as part of a superlattice-II type state [8].

In conclusion, we have shown that with weak damping the "broken" symmetries of time translation, time reversal, and Hamiltonian structure impose significant constraints on the equations describing SW near onset. These include scaling laws of resonant interactions with f_m and f_n, harmonic dependence on ϕ_f, and the dynamically significant preference for resonant coefficients of opposite sign in the 2MR problem. We have verified numerically these predictions for the Zhang-Viñals equations, and used them to interpret experimental results - they explain the oscillations seen with varying temporal phase in [4, 5] and predict the correct region of parameter space for 2MS states. We note, however, that it is not always clear whether the damping in a given experiment is "small enough" for our results to apply. This is particularly true when shallow containers are used and the damping due to boundary layer effects is important. It is unclear as well whether some procedures (such as the simple Taylor expansion in γ) would carry over to the full problem (Navier-Stokes equations with realistic boundary conditions) where the addition of damping constitutes a singular perturbation.

Finally, we emphasize that the ideas developed in this letter can be fruitfully applied to a variety of other patterns, and could be extended to include more general periodic forcing functions. In particular, they indicate how one might control resonant wave interactions (and hence pattern formation) through a judicious choice of the harmonic content of the forcing function. Furthermore, many aspects of our mathematical framework, developed here for parametrically excited SW patterns, should carry over to other problems in which TW naturally occur, e.g. via Hopf bifurcation. It would be interesting, for instance, to apply our framework to the problem of SW pattern control via weak temporal modulation of the control parameter [15, 16].

We thank J. Fineberg, M. Golubitsky, H. Riecke, C. Topaz, and P. Umbanhowar for helpful discussions. This work was supported by NASA grant NAG3-2364 and NSF grant DMS-9972059.

* Electronic address: jport@northwestern.edu

[1] M. C. Cross and P. C. Hohenberg, Rev. Mod. Phys. **65**, 851 (1993), and references therein.
[2] M. Golubitsky and D. G. Shaeffer, *Singularities and Groups in Bifurcation Theory, Volume I* (Springer-Verlag, New York, 1985).
[3] J. W. Swift, Nonlinearity **1**, 333 (1988).
[4] W. S. Edwards and S. Fauve, J. Fluid Mech. **278**, 123 (1994).
[5] A. Kudrolli, B. Pier, and J. P. Gollub, Physica D **123**, 99 (1998).
[6] H. Arbell and J. Fineberg, Phys. Rev. Lett. **81**, 4384 (1998).
[7] H. Arbell and J. Fineberg, Phys. Rev. Lett. **84**, 654 (2000).
[8] H. Arbell and J. Fineberg (2001), nlin.PS/0107072.
[9] W. Zhang and J. Viñals, J. Fluid Mech. **336**, 301 (1997).
[10] M. Silber, C. Topaz, and A. C. Skeldon, Physica D **143**, 205 (2000).
[11] J. Porter and M. Silber (2002), in preparation.
[12] For all m:n pairs tested (more than 10) the numerical calculations confirm our predictions with the exception of 3:4, where the term given in Eqs. (7) seems to be absent, giving way to one of higher order. This disagreement could be due to inadequate numerical resolution, or to a hidden symmetry of some kind.
[13] P. Chossat, Dynam. Cont. Dis. Ser. A **8**, 575 (2001).
[14] D. Armbruster, J. Guckenheimer and P. Holmes, Physica D **29**, 257 (1988); J. Guckenheimer and A. Mahalov, Physica D **54**, 267 (1992); J. Porter and E. Knobloch, Physica D **159**, 125 (2001).
[15] H. Riecke, J. D. Crawford, and E. Knobloch, Phys. Rev. Lett. **61**, 1942 (1988).
[16] M. Dennin, Phys. Rev. E **62**, 7842 (2000).